This document is the Accepted Manuscript version of a Published Work that appeared in final form in APPLIED SURFACE SCIENCE, copyright © Elsevier Ltd after peer review and technical editing by the publisher. To access the final edited and published work see [https://doi.org/10.1016/j.apsusc.2021.150377]
Licence CC BY-NC-ND

Highly conductive and transparent graphene: synergy of covalent and non-covalent co-doping.

Giuseppe Valerio Bianco[a]* Alberto Sacchetti[a], Marco Grande,[a,b] Antonella D'Orazio[b] , Pio Capezzuto,[a] and Giovanni Bruno.[a]

[a]*CNR-NANOTEC, Dept. of Chemistry, Univ. of Bari. Via Orabona, 4-70123 Bari, Italy*

[b] *Dipartimento di Ingegneria Elettrica e dell'Informazione, Politecnico di Bari; via Orabona,4 - 70123 Bari, Italy*

*Contacting author. Email: giuseppevalerio.bianco@cnr.it

Abstract

The three values of transparency, conductivity and flexibility make graphene a valid alternative to replace traditional electrode materials such as indium tin oxide in electrical and optical devices. In recent years, research efforts have been addressed to investigate doping methodologies for reducing further the sheet resistance while maintaining high transparency.

In this contribution, we explore the possibility to integrate both the covalent and non-covalent doping in order to increase the carrier charge density without affecting their mobility significantly. We present a new graphene doping methodology that combines the effect of $SOCl_2$ covalent p-doping with a synergic p-doping effect of cationic gold nanoparticles activated by the same $SOCl_2$ chemistry. We demonstrate that this original co-doping strategy can provide CVD graphene multilayers with record sheet resistance Rs performances, which meet the technical target required by several industrial applications.

1. Introduction

Nowadays, there is no doubt that the success of graphene is related to the unique combination of its electrical, optical, mechanical and thermal properties, and certainly for the main reason of being an atomic layer material resembling an "infinite molecule". However, it is also true that the development of technological applications of graphene requires the parallel development of effective methods of functionalization of the graphene. Among the many possible applications demonstrated in recent years,

an important area is in the optoelectronic field where the two parameters of optical transparency and high conductivity enables graphene to enter, as the last "wonderful" member, in the family of transparent conductive materials. Nevertheless, the use of graphene as a transparent conductive layer (TCL) has not yet reached full maturity and in many applications the existing materials, e.g. transparent conductive oxides, e.g. ITO and AZO, remain competitive [1-6].

Thus, while the processes of synthesis of graphene on a large area have reached satisfactory levels in terms of both production technology and of material quality, we still have some major challenges in graphene functionalization research. Therefore, functionalization methodologies, both covalent and non-covalent, that can positively modify the transport properties are critical for applications [7-12]. From a general point of view, the interaction of graphene with atoms or molecules leads to modifications of the π-conjugation, and then to the change of the electron density and thus the transport properties. The functionalization via covalent reaction often occurs through rehybridization from sp^2 to sp^3, but also through passivation of dangling bonds and by replacing contaminant atoms. Summarizing, the chemical reactivity of graphene has origin from: -*i*) intrinsic reactivity associated to the delocalized π-bonds; -*ii)* the edges, both zig-zag and armchairs, of the graphene grains; -*iii)* the carbon vacancies that arise dangling bonds inside the basal plane; -*iv*) local structural defects, e.g. Stone-Wales defects, that originate curvature in the graphene sheet, i.e. out of plane C-atoms; -*v*) contamination species (OH, CO, COOH) [13-17]. The non-covalent functionalization is realized by adsorption/deposition of particles and molecules with a very different work function thus activating the electron transfer from/to graphene [7,8,10,18-20].

In working towards this aim, we have investigated “new” doping procedures with a view to reduce the sheet resistance strongly well below the limit value reported in literature [21-24]. In the present paper, we have explored the possibility to integrate both the covalent and non-covalent doping in order to increase the carrier charge density without affecting their mobility significantly and, hence, with an increase of conductivity. Specifically, the $SOCl_2$ covalent doping, already investigated in our previous study [24] under both thermal and pyridine-catalyzed (“organic aqua-regia” [25, 26]), is coupled with the redox (Au^{3+}/Au) non-covalent doping.

2. Experimental

Large-area monolayer graphene was grown by chemical vapour deposition on 25 μm thick Cu foils (Alfa Aesar, item No. 13382), and transferred onto both Corning glass and 300 nm SiO_2 / Si substrates (p^+-doping, resistivity ~0.002÷0.005 Ohm cm) using the thermal release tape methodology similar to that reported in ref. [24]. Prior to deposition of the gold nanoparticles (np-Au), the quality of

pristine graphene is evaluated by Raman spectra, Sheet resistance and field effect (FET) measurements (see Figures S1 and S2 in Supplementary Information).

Gold (np-Au) deposition was performed in a hot wire evaporator system (Balzers Union, MED010) with a base pressure of better than 10^{-5} mbar. A high-purity (99.9999%) Au wire was wound across the tungsten filament at the top of the vacuum chamber and DC resistive heating evaporated the Au. By adjusting the heating current and the evaporation time, it was possible to control coverage and, therefore, the size of the Au nanoparticles.

The doping procedure of graphene/Au layers with $SOCl_2$, also in presence of pyridine, was carried out using the same glass-autoclave described in ref. [24]. For thermal activation reaction, the glass-autoclave was heated in an oven at temperature of about 140°C for a time of 60 min. For the pyridine-catalysed process at room temperature, 15 min are enough to complete the doping process.

Supplementary graphene layers were directly transferred onto the np-Au/doped graphene samples by hot-pressing of the graphene/TR-tape (at 100°C) thus releasing the tape.

The effectiveness of the doping procedure was evaluated by the use of Raman spectroscopy and sheet resistance measurements. Raman spectra were recorded with a LabRam HR (Horiba JY) system. All spectra were measured at room temperature with 532 nm laser light and captured using 100x objective lens magnification with a focusing laser spot less than 1μm in diameter. The laser power was kept at 1.0 mW to avoid laser-induced heating effect. The sheet resistance measurements were carried out with a Keithley 2400 Source Meter, using a home-built 4-probe Van der Pauw configuration system. The value was averaged over the five data points at different location for each sample.

3. Results and Discussion

For investigating the covalent and non-covalent holes-codoping effect on the transport properties of CVD graphene, monolayer graphene on Corning glass substrates was covered with gold nanoparticles by thermal evaporation and finally treated with $SOCl_2$ (thermally or pyridine-catalysed). The scheme of the device and the chemistry of the doping are illustrated in Figure1**.**

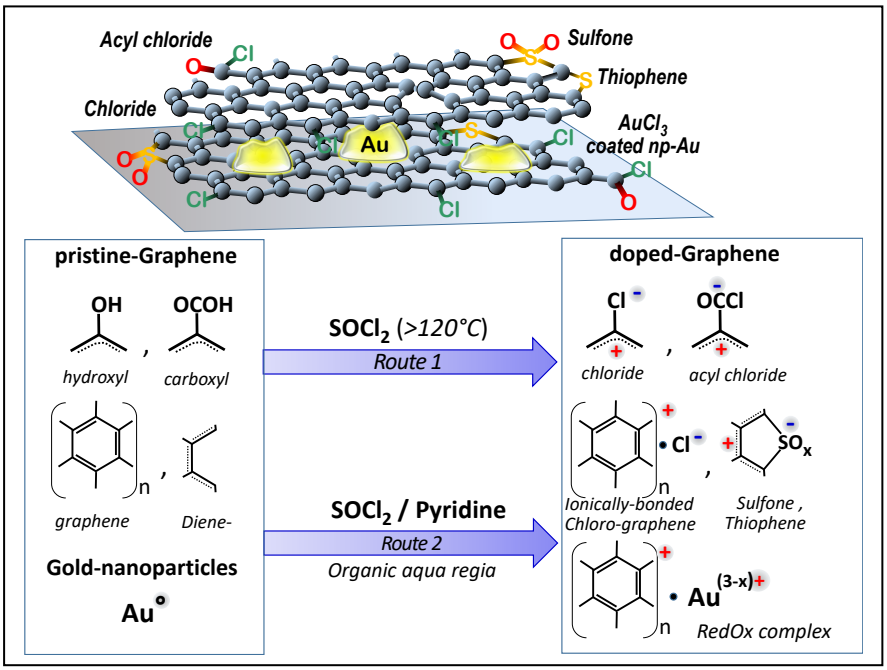

Figure 1. Schematic representation of the assembled graphene bilayer with intercalated gold nanoparticles after $SOCl_2$ doping. The involved doping chemistry under both thermal activation @ T>120 °C (route 1) and pyridine-catalysed (route 2) is summarized by the main functionalities involved in the covalent and non-covalent doping process.

The figure shows the gold nanoparticles (np-Au) covered with the $AuCl_3$ shell and sandwiches between two layers of functionalized-graphene. The formation of $AuCl_3$ and of chlorine- and sulphur-functionalized graphene results from the treatment with $SOCl_2$ under thermal or pyridine-catalyzed ("organic aqua-regia") conditions**.** The chemistry of graphene doping processes following $SOCl_2$ treatment has been described in a previous publication [24]. As for the oxidation of metallic gold to Au_3^+, the involved chemical processes are illustrated in Figure 2.

Thermal Oxidation of Metallic Gold by Thionyl Chloride (T ≥120°C)

$$2\ SOCl_2 \rightleftharpoons SCl_2 + SO_2 + Cl_2 \qquad (1)$$

$$2\ Au + 3\ Cl_2 \longrightarrow 2\ AuCl_3 \qquad (2)$$

Catalytic Oxidation of Metallic Gold by "Organic Aqua Regia" (RT)

$$2\ Au + 3\ SOCl_2 \xrightarrow[pyridine]{N} 2\ AuCl_3 + 3\ SO \qquad (3)$$

Figure 2. Chemistry of the oxidation of metallic gold (Au) to gold chloride ($AuCl_3$) by thionyl chloride under thermal and catalytic conditions.

In the case of $SOCl_2$ thermal treatment, the process starts with the decomposition of $SOCl_2$ (eq.1) at temperature higher than 120°C thus producing chlorine (Cl_2) for the subsequent reactive chemisorption (eq. 2) on gold surface to gold chloride ($AuCl_3$) [27, 28]. Whereas, in the case of pyridine-catalysed process, the formation of a charge-transfer complex between pyridine and $SOCl_2$ (partial transfer of the electron density on the nitrogen to the sulphur) activates $SOCl_2$ to oxidize Au (eq.3) [25, 26]. Thus, while $SOCl_2$ alone cannot oxidize Au, it turns out to be a strong oxidant when at high temperature or in presence of pyridine. Raman spectra confirm that the structure of the resulting superficial oxidized gold is similar to the gold (III) chloride (see Figure S3 in Supplementary Information).

Many researchers [29-33] have described the role of metal ions, as n- and p-dopant of graphene in a redox reaction. Among others, Shi et al. [29] described the effect of $AuCl_3$ doping time on the surface morphology of Au nanoparticles and surface potential of graphene by spontaneous reduction of Au^{3+} ion. The specificity of the redox complex between graphene and ionized gold relies on electrochemical consideration, since the reduction potential of Au^{3+} ion (1.0 V) is higher than the reduction potential of graphene (0.2 V) [29]. Thus, the redox process takes place on graphene surface with an electron transfer from graphene to Au^{3+} resulting in a p-doping behaviour of graphene while Au^{3+} ions are reduced towards lower ionization ($Au^{(3-x)+}$) up to metallic Au. Consequently, the Fermi level shifts well below the Dirac point.

The quality and the characteristic features of p-doping process were studied by optical transmittance, Raman spectroscopy, and sheet resistance measurements.

To monitor the Au nanoparticles formation, we measured the evolution of the transmittance spectra as illustrated in Figure 3.

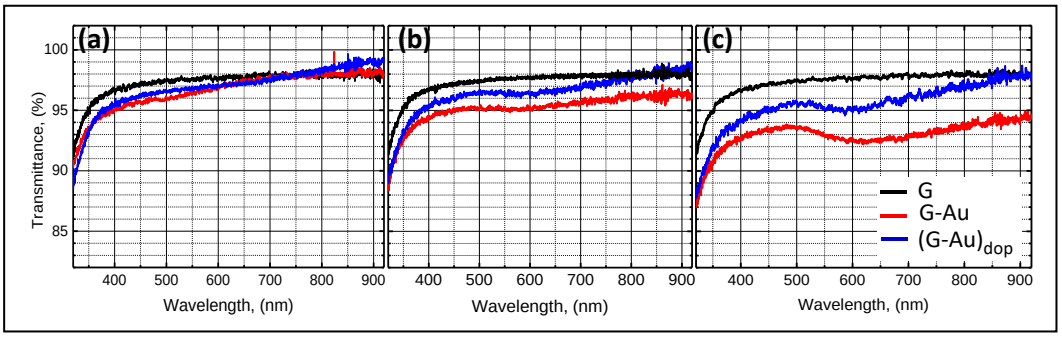

Figure 3. Optical transmission spectra of the single layer graphene coated with increasing amount of gold nanoparticles depending on the evaporation exposure time of 3 sec (a), 5 sec (b) and 7 sec (c). The growth of the surface-plasmon absorption band (red line) indicates the production of increasing size of gold nanoparticles on pristine graphene. The blue curve is the transmittance measured after the $SOCl_2$ doping.

The UV-Vis spectra of the graphene on Corning glass samples were measured before, G, and after gold deposition, G-Au, and after $SOCl_2$ doping, $(G\text{-}Au)_{dop}$. In figure 3 three typical samples with increasing amount of gold on single layer graphene are shown. As can be seen, the increased amount of gold is evidenced by the lowering of transmittance (red curve) but also by the characteristic plasmon resonance band for gold nanoparticles centred at about 600 nm for the sample with 7 sec of gold evaporation time (Figure 3c). Visually we observe a slightly increase of the plasmon peak with increasing amount of evaporated gold. It is important to note that the samples, after $SOCl_2$ doping, are more transparent (blue curve) than before doping (red curve). This is ascribed to the gold chlorination and hence to the formation of $AuCl_3$ shell on the gold nanoparticles.

Next, we investigated the doping effectiveness of the prepared samples by Raman spectroscopy. Figure 4 shows the representative Raman spectra acquired during the different preparation steps of the single layer graphene doped covalently and non-covalently. Figure 4a shows the spectra of pristine graphene (black-line spectra) and Au-covered graphene before (red-line spectra) and after (blue-line spectra) $SOCl_2$ doping. Importantly, the D-peak at ≈1350 cm^{-1}, i.e. the peak related to the presence of sp^3-carbon defects, is undetectable thus indicative of the absence of a significant number of defects. The G-peak of pristine graphene, centred at 1586 cm^{-1} with a full-width at half-maximum (FWHM) of 14 cm^{-1}, shows a symmetric Lorentzian shape, whereas after np-Au deposition the G-band shows a red shift with an asymmetrical profile (see Figure 4b) that can be fitted by two Lorentzian sub-peaks as shown in Figure 4d. Specifically, the G1 and G2 peak at, respectively, 1574 cm^{-1} and 1588 cm^{-1}, indicative of two different scattering processes, could be due to strain, doping or both effects. The G-band asymmetry has been observed by others and attributed to localized charge inhomogeneity within the laser probe, i.e., on a scale of less than 1μm [34].

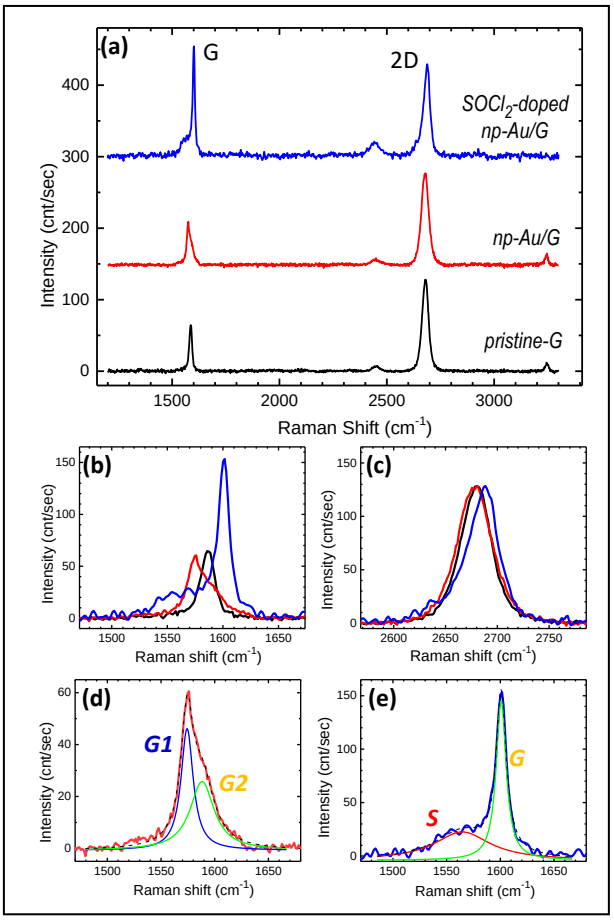

Figure 4. Raman characterization of single layer graphene before and after $SOCl_2$ doping. (a) Raman spectra of pristine-graphene single layer on Corning-glass (black line), after np-Au deposition (red line) and after $SOCl_2$ chemical doping (blue line). (b) and (c) Details of the G and 2D peaks, respectively, showing their shift following the np-Au deposition and $SOCl_2$ doping. (d) DE convolution in two peaks (Lorentzian analysis) of the G peak of the pristine grapheme after np-Au deposition. The G-peak splitting and the red-shift of the G1 peak (1574 cm^{-1}) with respect to G2 (1586 cm^{-1}), is evidence of the localized n-type doping due to np-Au. (d) Two Lorentzian curve fitting of the G peak after $SOCl_2$ doping. The large peak S at 1558 cm^{-1}, confirms the presence of disordered sp^2-carbon attributed to the chemical defects by large functional atoms such as chlorine and sulphur.

The most frequent observation of G-peak splitting is en-countered when graphene is submitted to uniaxial strain [35-37]. However, it has been reported that the strain-related splitting and red-shift of the G peak is accompanied by the parallel 2D peak red-shift that is 2 times higher than the G-peak shift [38]. What we observe following the deposition of the np-Au is an almost negligible red shift of the 2D peak (see Figure 4c), whereas the shift (red peak in Figure 4b) and splitting (Figure 4d) of the related G band is significant. This means that rather than strain, the dominant cause of the G-peak splitting is likely to

be the inhomogeneous doping resulting from np-Au coverage. The explanation of the correlation of G-peak splitting and doping may rest on the observed red-shift of the G1-peak to 1574 cm-1 that is due to localized n-type doping of graphene covered with gold nanoparticles [39]. Here, it is important to underline that pristine CVD-graphene is already p-doped as confirmed by FET measurements (see Figure S3 in Supplementary Information). This unintentionally p-doping of graphene as transferred on Corning glass or SiO_2/Si substrates and exposed to air is mostly due to chemical defects at the grain boundaries, adsorbates and charge transferring to the substrate. In fact, pristine graphene typically presents sheet resistance in the range 500-1200 Ohm/square. Thus, the red shift of the G1-peak may be explained by the reduced hole density due to carrier compensation effect of n-doping by gold nanoparticles [39].

Following the chemical doping process with thionyl chloride ($SOCl_2$), significant changes occur in the frequencies, intensities and widths of the Raman band (blue line spectra in Figure 4). The decrease of 2D/G peaks ratio to less than 1 (see Figure 4a), the blue-shift of both G and 2D peaks at, respectively, 1600 $cm^{-1}$and 2678 cm^{-1} (see Figures 4b and 4c), and the narrowing of G peaks to 10 cm^{-1} are characteristic of a strong p-doping of graphene, which corresponds to an upshift of the fermi level of ~0.5 eV [40]. Similarly, to that previously observed for $SOCl_2$-doping of graphene [24] the Raman spectra of $SOCl_2$-doped np-Au/Graphene shows a wide shoulder on the left side of the G-peak (see Figure 4a). Thus, the wide peak S at about 1558 cm^{-1} (Figure 4e) confirms the presence of disordered sp^2-carbon attributed to the chemical defects by large functional atoms such as chlorine and sulphur [41, 42].

The amount of doping, following the $SOCl_2$ treatment of the np-Au/Graphene layer, has pronounced effects on the electrical conductivity of the sample. Figure 5 presents the variation of sheet resistance and of optical transmittance at the different preparation steps of the doped graphene gold graphene window layer. Following the first doping on single layer graphene/np-Au, the second layer of graphene is transferred and then doped again.

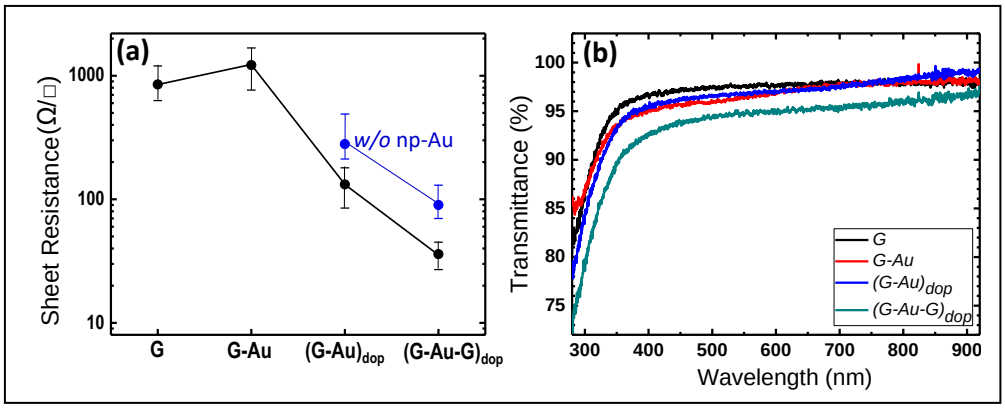

Figure 5. (a) Sheet resistance data of a bilayer graphene device on Corning glass following the three preparation steps of $SOCl_2$ doping with (black line) and without (blue line) np-Au. (b) Optical transmittance spectra of the graphene device following the preparation steps.

An interesting feature is the slight increase of sheet resistance observed at the first step of deposition of np-Au on the pristine graphene. This behaviour of the sheet resistance confirms the n-doping effect of the np-Au as already observed by the red shift and splitting of G-peaks in the Raman spectrum (see Figures 4b, 4d). The data show that the graphene doped with $SOCl_2$ including the np-Au, i.e. including the electron withdrawing Au^{3+} ions, can realize a significantly lower sheet resistance than the graphene without np-Au. Specifically, the G-Au-G "sandwich" shows the sheet resistance of about 35 Ω/□, which is almost equivalent to the value that is obtained with a 4-layer doped graphene [21, 24]. Nevertheless, the optical transmittance performance of the double layer is not affected significantly, as long as the np-Au coating is very low, which is the case shown in Figures 5b, where the loss of transmittance is less than 1% compared to a double layer without np-Au. Interestingly, we noticed that the slight increase of gold amount by the control of the evaporation time affected the optical transparency (see Figures 3) without any significant influence on the sheet resistance. Furthermore, the p-doped double layer graphene not only show low sheet resistance and transparency but also maintain the doping effect even after in-air exposure and high temperature. The peculiarities on the stability of doping have been described in our previous study (ref. 24). The performances of our transparent doped bilayer can further be improved by the addition of a third undoped cover layer, which causes a reduction in transmittance of 2.3 % with no effect in sheet resistance that remains stable for months.

These results, i.e. the good T/Rs figure of merit, show that the synergistic doping methodology proposed in this study is a promising approach for graphene-based transparent electrodes. Moreover, the presence of plasmonic enhanced light absorption/scattering of gold nanoparticles might offer great potential in photovoltaic applications

4. Conclusions

We have demonstrated the possibility to combine covalent and non-covalent doping of graphene aimed at decreasing the sheet resistance while maintaining high transparency of the conductive layer.

The covalent p-doping realized by the chlorination of graphene using $SOCl_2$, previously investigated in our lab, has been performed on graphene layer covered with gold nanoparticles (np-Au). Our results indicate that $SOCl_2$, when at temperature higher than 120 °C or in presence of pyridine, induces the

oxidation of np-Au into Au^{3+} ions on graphene leading, subsequently, to the redox process by which electrons transfer from graphene to Au^{3+} ions and, consequently, to a more effective p-doping of graphene.

The results of this study provide important elements for the validation of the synergy of doping methods in reducing the sheet resistance and thus in making competitive graphene layers as transparent conductor (TCL).

5. Acknowledgements

Authors acknowledge the GraFoMi project (2019-2021), funded by Politecnico di Bari (Italy)

6. References

1. A.C. Ferrari et al. *"Science and technology roadmap for graphene, related two dimensional crystals, and hybrid systems"*. Nanoscale, 7(11) (2015) 4598-4810.
2. J. Jo, J.U. Lee, W.H. Jo, "*Graphene-based electrodes for flexible Electronics*", Polym. Int. 64 (2015) 1676-1684.
3. K.S. Kim, Z. Yue, H. Jang, S.Y. Lee, J.M. Kim, K.S. Kim, J.-H. Ahn, P. Kim, J.-Y. Choi, B.H. Hong, "*Large-scale pattern growth of graphene films for stretchable transparent electrodes"*, Nature 457 (2009) 706-710.
4. Y. Zhu, Z. Sun, Z. Yan, Z. Jin, J.M. Tour, *"Rational design of hybrid graphene films for high-performance transparent electrodes",* ACS Nano 5 (8) (2011) 6472-6479.
5. Hyesung Park, Patrick R. Brown, Vladimir Bulović, and Jing Kong, *" Graphene As Transparent Conducting Electrodes in Organic Photovoltaics: Studies in Graphene Morphology, Hole Transporting Layers, and Counter Electrodes",* Nano Lett., 12 (2012) 133−140.
6. T. Cui, R. Lv, Z-H Huang, S. Chen, Z. Zhang, X. Gan, Y. Jia, X. Li, K. Wang, D. Wua and F. Kang, "*Enhanced efficiency of graphene/silicon heterojunction solar cells by molecular doping*", J. Mater. Chem. A, 1, (2013) 5736–5740.
7. H. Leea, K. Paengb, I. S. Kima. "*A review of doping modulation in graphene"*. Synthetic Metals 244 (2018) 36–47.
8. H. Liu, Y. Liu and D. Zhua. "*Chemical doping of graphene*", J. Mater. Chem., 21 (2011) 3335–3345 .

9. V. Georgakilas, M. Otyepka, A. B. Bourlinos, V. Chandra, N. Kim, K. C. Kemp, P. Hobza, R. Zboril, and K. S. Kim. "*Functionalization of Graphene: Covalent and Non-Covalent Approaches, Derivatives and Applications"*. Chem. Rev., 112 (2012) 6156−6214.
10. Y. Kim, J. Park, J. Kang, J. M. Yoo, K. Choi, E. Sun Kim, J-B. Choi, C. Hwang, K. S. Novoselov and B. H. Hong. *"A highly conducting graphene film with dual-side molecular n-doping.",* Nanoscale, 6 (2014) 9545–9549.
11. Luis M. Arellano, Sun Yue, Pedro Atienzar, Marı J. Go´mez-Escalonilla, Francisco J. Ortega-Higueruelo, Jose´ Luis G. Fierro, Hermenegildo Garcı and Fernando Langa, "*Modulating charge carrier density and mobility in doped graphene by covalent functionalization"*. Chem. Commun., 55 (2019) 9999—10002.
12. J. K. Wassei, K. C. Cha, V. C. Tung, Y. Yang and R. B. Kaner, "*The effects of thionyl chloride on the properties of graphene and graphene–carbon nanotube composites"* J. Mater. Chem., 21 (2011) 3391.
13. P. A. Denis and F. Iribarne, *"Comparative Study of Defect Reactivity in Graphene",* J. Phys. Chem. C , 117 (2013) 19048−19055. .
14. G. Yang, L. Li, W. B. Lee, and M. Cheung Ng. *"Structure of graphene and its disorders: a review",* Science and Technology of Advanced Materials, 19 (2018) 613-648.
15. V. A. Tur1, A. V. Okotrub, Yu. V. Shubin, B. V. Senkovski, and L. G. Bulusheva, *"Chlorination of perforated graphite via interaction with thionylchloride"*, Phys. Status Solidi B, 251(12) (2014) 2613–2619.
16. T. Schiros, D. Nordlund, L. Pálová, D. Prezzi L. Zhao, K. S. Kim, U. Wurstbauer, C. Gutiérrez, D. Delongchamp, C. Jaye, D. Fischer, H. Ogasawara, L. G. M. Pettersson, D. R. Reichman, P. Kim, M. S. Hybertsen, and A. N. Pasupathy, *"Connecting Dopant Bond Type with Electronic Structure in N-Doped Graphene"*, Nano Lett., 12 (2012) 4025−4031.
17. R. Singla, A. Kottantharayil, "*Stable hydroxyl functionalization and p-type doping of graphene by a non-destructive photo chemical method*", Carbon 152 (2019) 267-273.
18. Y-M Seo, W. Jang, T. Gu and D. Whang. "*Highly Efficient n-Type Doping of Graphene by Vacuum Annealed Amine-Rich Macromolecules*", Materials, 13 (2020) 2166.
19. V. P. Pham, K. N. Kim, M. H. Jeon, K. S. Kimb and G. Y. Yeom, "*Cyclic chlorine trap-doping for transparent, conductive, thermally stable and damage-free Graphene"*, Nanoscale, 6 (2014) 15301–15308.
20. A. Kasry, M. A. Kuroda, G. J. Martyna, G. S. Tulevski, and A. A. Bol. *Chemical Doping of Large-Area Stacked Graphene Films for Use as Transparent, Conducting Electrodes*. ACS Nano, 4 (7) (2010).

21. S. Bae, H. Kim, Y. Lee, X. Xu, J.-S. Park, Y. Zheng, J. Balakrishnan, T. Lei, H. R. Kim, Y. I. Song, Y.-J. Kim, K. S. Kim, B. Özyilmaz, J.-H. Ahn, B. Hee Hong, and S. Lijima, *"Roll-to-roll production of 30-inch graphene films for transparent electrode".* Nature Nanotechnology, 5 (2010) 574–578.
22. F. Gunes, H. J. Shin, C. Biswas, G. H. Han, E. S. Kim, S. J. Chae, J. Y. Choi, and Y. H. Lee, "*Layer-by-Layer Doping of Few-Layer Graphene Film"*, ACS Nano 4 (2010) 4595–4600.
23. J. Kang, H. Kim, K. S. Kim, S. K. Lee, S. Bae, J. H. Ahn, Y. J. Kim, J. B. Choi, and B. H. Hong, "*High-Performance Graphene-Based Transparent Flexible Heaters"*, Nano Lett., 11(2011) 5154–5158.
24. G. V. Bianco, A. Sacchetti, A. Milella, M. Grande, A. D'Orazio, P. Capezzuto, G. Bruno. "*Extraordinary low sheet resistance of CVD graphene by thionyl chloride chemical doping".* Carbon 170 (2020) 75-84.
25. W. Lin, R. W. Zhang, S. S. Jang, C. P. Wong, and J. I. Hong, *"Organic Aqua Regia - Powerful Liquids for Dissolving Noble Metals"*, Angew. Chem. Int. Ed., 49 (2010) 7929-7932.
26. W. Lin, "*Organic Aqua Regia: Discovery, Fundamentals, and Potential Applications", Noble Metals*, Yen-Hsun Su, IntechOpen, (2012), DOI: 10.5772/33661.
27. N. D. Spencer, R. M. Lambert, *"Chlorine Chemisorption and Surface Chloride Formation on Au(111)"* Surf. Sci. 107, (1981) 237-248.
28. G. N. Kastanas and B. E. Koel. "*Interaction of Cl_2, with the Au(111) surface in the temperature range of 120 to 1000 K".* Applied Surface Science 64 (1993) 235-249.
29. Y. Shi, K. K. Kim, A. Reina, M. Hofmann, L.-J. Li and J. Kong "*Work Function Engineering of Graphene Electrode via Chemical Doping",* ACS Nano, 4 (5) (2010) 2689–2694.
30. K. K Kim, R. R. Alfonso, Y. Shi, H. Park, L.-J. Li, Y. H. Lee, J. Kong, " *Enhancing the conductivity of transparent graphene films via doping*", Nanotechnology 21 (2010) 285205.
31. D. Zhan, L. Sun, Z. H. Ni, L. Liu, X. F. Fan, Y. Wang, T. Yu, Y. M. Lam, W. Huang and Z. X. Shen "*FeCl 3 -Based Few-Layer Graphene Intercalation Compounds: Single Linear Dispersion Electronic Band Structure and Strong Charge Transfer Doping",* Adv. Funct. Mater., 20 (2010).
32. K. C. Kwon, K. S. Choi, and S. Y. Kim "*Increased Work Function in Few-Layer Graphene Sheets via Metal Chloride Doping",* Adv. Funct. Mater. 22, (2012), 4724–4731.
33. K. C. Kwon, K. S. Choi, C. Kim, and S. Y. Kim, "*Role of Metal Cations in Alkali Metal Chloride Doped Graphene"*, J. Phys. Chem. C 118 (2014) 8187−8193.
34. C. Casiraghi, S. Pisana, K. S. Novoselov, A. K. Geim, and A. C. Ferrari, "*Raman fingerprint of charged impurities in graphene* ". Appl. Phys. Lett., 91 (2007) 233108.

35. Y. Zhang, C. Luo, W. Lia and C. Pan. "*Strain induced chemical potential difference between monolayer graphene sheets"* Nanoscale, 5 (2013) 2616.
36. A. C. Ferrari and D. M. Basko, *"Raman spectroscopy as a versatile tool for studying the properties of graphene"* Nature Nanotechnology. 8 (2013) 235-246.
37. J. Vejpravova, B. Pacakova, J. Endres, A. Mantlikova, T. Verhagen, V. Vales, O. Frank and M. Kalbac *"Graphene wrinkling induced by monodisperse nanoparticles: facile control and quantification",* Scientific Reports 5 (2015) 15061.
38. T. M. G. Mohiuddin, A. Lombardo, R. R. Nair, A. Bonetti, G. Savini, R. Jalil, N. Bonini, D. M. Basko, C. Galiotis, N. Marzari, K. S. Novoselov, A. K. Geim, and A. C. Ferrari, " *Uniaxial strain in graphene by Raman spectroscopy: G peak splitting, Grüneisen parameters, and sample orientation*", Physical Review B, 79 (2009) 205433.
39. Y. Wu, W. Jiang, Y. Ren, W. Cai, W. H. Lee, H. Li, R. D. Piner, C. W. Pope, Y. Hao, H. Ji, J. Kang, and R. S. Ruoff, "*Tuning the Doping Type and Level of Graphene with Different Gold Confi gurations* ", Small *8* (20) (2012) 3129–3136.
40. A. Das, S. Pisana, B. Chakraborty, S. Piscanec, S. K. Saha, U. V. Waghmare, K. S. Novoselov, H. R. Krishnamurthy, A. K. Geim, A. C. Ferrari, and A. K. Sood, "*Monitoring dopants by Raman scattering in an electrochemically top-gated graphene transistor*", Nature Nanotechnology, 3 (2008) 210-215.
41. A. Sadezky, H. Muckenhuber, H. Grothe, R. Niessner, and U. Poschl, *"Raman microspectroscopy of soot and related carbonaceous materials: Spectral analysis and structural information*", Carbon, 43 (2005) 1731–1742.
42. N. Li, Z. Wu, Lei Huo, L. Zong, Yujie Guo, J. Wang, and X. Ji,*"One-step functionalization of carbon fiber using in situ generated aromatic diazonium salts to enhance adhesion with PPBES resins",* RSC Adv., 6 (2016) 70704-70714.